Analysis of finite difference discretization schemes for diffusion in spheres with variable diffusivity

Citation: Ford Versypt, Ashlee N., and Richard D. Braatz. "Analysis of Finite Difference Discretization Schemes for Diffusion in Spheres with Variable Diffusivity." Computers & Chemical Engineering 71 (2014): 241–252.

As Published: http://dx.doi.org/10.1016/j.compchemeng.2014.05.022

Publisher: Elsevier

Persistent URL: http://hdl.handle.net/1721.1/106943

Version: Author's final manuscript: final author's manuscript post peer review, without publisher's formatting or copy editing

Published in final edited form as:
Comput Chem Eng. 2014 December 4; 71: 241–252. doi:10.1016/j.compchemeng.2014.05.022.

Analysis of Finite Difference Discretization Schemes for Diffusion in Spheres with Variable Diffusivity

Ashlee N. Ford Versypt[a] and **Richard D. Braatz**[a,*]

[a]Department of Chemical Engineering, Massachusetts Institute of Technology, Cambridge, MA 02139, USA

Abstract

Two finite difference discretization schemes for approximating the spatial derivatives in the diffusion equation in spherical coordinates with variable diffusivity are presented and analyzed. The numerical solutions obtained by the discretization schemes are compared for five cases of the functional form for the variable diffusivity: (I) constant diffusivity, (II) temporally-dependent diffusivity, (III) spatially-dependent diffusivity, (IV) concentration-dependent diffusivity, and (V) implicitly-defined, temporally- and spatially-dependent diffusivity. Although the schemes have similar agreement to known analytical or semi-analytical solutions in the first four cases, in the fifth case for the variable diffusivity, one scheme produces a stable, physically reasonable solution, while the other diverges. We recommend the adoption of the more accurate and stable of these finite difference discretization schemes to numerically approximate the spatial derivatives of the diffusion equation in spherical coordinates for any functional form of variable diffusivity, especially cases where the diffusivity is a function of position.

Keywords

finite difference method; variable coefficient; diffusion; spherical geometry; method of lines

1. Introduction

Variable diffusivity is important in physical and chemical systems such as in the diffusion of moisture during the drying or wetting of food products (e.g., legumes, tomatoes, and porous baked goods) that have concentration-dependent water diffusivity (Hsu, 1983; Tong and Lund, 1990; Xanthopolous et al., 2012), the diffusion of acid through chemically-amplified resist materials undergoing photolithography where the diffusivity depends on the extent of the chemical reactions (Petersen et al., 1995), and the diffusion of medicines through drug-loaded, biodegradable polymer microspheres that have internal porosity that changes with

*Corresponding author at: 77 Massachusetts Ave., MIT 66-372, Cambridge, MA 02139, USA. Tel.: +1 617 253 3112; fax: +1 617 258 0546. braatz@mit.edu. .

chemical degradation thus modifying the effective diffusivity of the drug (Ford Versypt et al., 2013; Ford et al., 2011; Ford Versypt, 2012). Both the food product wetting/drying and polymer microsphere drug delivery examples of variable diffusivity involve diffusion through a spherical domain.

The partial differential equation (PDE) for Fickian diffusion within a radially symmetric sphere is

$$\frac{\partial c}{\partial t}=\frac{1}{r^2}\frac{\partial}{\partial r}\left(r^2\frac{D}{R^2}\frac{\partial c}{\partial r}\right), \quad (1)$$

where $c(r,t)=\hat{c}(r,t)/\hat{c}(0,0)$ is the dimensionless concentration of the diffusing species, $\hat{c}(r,t)$ is the concentration, $\hat{c}(0,0)$ is the initial concentration at the center of the sphere, $r=\hat{r}/R$ is the normalized radial position, $\hat{r}$ is the the radial distance from the center of the sphere, R is the radius of the sphere, t is time, and $D(r, t)$ is the effective diffusivity of the diffusing species in the medium. The parameter $\alpha(r, t) = D(r, t)/R^2$ is used for simplifying the notation and is referred to as the "diffusivity" here.

For uniform initial concentration, the initial condition is

$$c(r,0)=1, \quad 0\leq r<1, \quad (2)$$

and for radial symmetry about the center of the sphere and constant surface concentration, the boundary conditions are

$$\frac{\partial c(0,t)}{\partial r}=0, \quad t\geq 0, \quad (3)$$

and

$$c(1,t)=0, \quad t\geq 0, \quad (4)$$

respectively.

The PDE (1) in spherical coordinates for mass transport by diffusion (or analogously for heat transport by conduction) with a constant diffusivity and the specified initial condition (2) and boundary conditions (3) and (4) is readily solved with analytical solutions (Crank, 1975; Carslaw and Jaeger, 1986). Some analytical and semi-analytical methods exist for solving the PDE (1) for diffusion with variable diffusivity in specific cases: concentration-dependent diffusivity with rectangular coordinates, e.g. (Crank, 1975; Ozisik, 1993; Tsang and Hammarstrom, 1987); concentration-dependent diffusivity with spherical coordinates for $D = f(\exp(c))$ (Hsu, 1983) and for $D = 1+f(c)$ (Renganathan and White, 2011), where f represents some linear or nonlinear function; and spatially-dependent diffusivity with rectangular coordinates (Zoppou and Knight, 1999). In the most general case of variable diffusivity with an arbitrary, nonlinear functional form, the PDE (1) in spherical coordinates is not separable, cannot be easily transformed into a simpler equation, and must be solved numerically.

A commonly used numerical method in engineering is the method of lines (Schiesser, 1991, 2013). The method of lines reduces the diffusion PDE (1) into a system of ordinary differential equations (ODEs) by discretizing the radial dimension onto a finite grid with equal spacing Δr and coordinates $r_i = i\Delta r$ for $i = 0, 1, \ldots, M$ using some finite difference discretization scheme (LeVeque, 2007). The resulting system of semi-discrete ODEs for the species concentration at each grid point can be solved using a standard ODE solver such as RADAU5, an implicit 4th-5th order Runge-Kutta solver with adaptive time-stepping (Hairer and Wanner, 1996), which is used here. The key decision in solving the diffusion PDE (1) numerically by this technique, or any numerical method involving spatial discretization, is in the choice of finite difference discretization scheme to handle the variable diffusivity term.

If the diffusivity has a constant value of α_0, the method of lines may be applied with the well-known, central finite difference discretization scheme in spherical coordinates. This scheme for numerically approximating the spatial derivatives of the diffusion equation (1) with second-order accuracy (for derivation see Appendix A.1) written in the ODE form for the method of lines is (Crank, 1975; Carslaw and Jaeger, 1986; Ozisik, 1993)

$$\frac{dC_i}{dt} = \begin{cases} \frac{6\alpha_0}{\Delta r^2}\left(C_1 - C_0\right), & \text{if} \quad i=0; \\ 0, & \text{if} \quad i=M; \\ \frac{\alpha_0}{i\Delta r^2}\left((i+1)\,C_{i+1} - 2iC_i + (i-1)\,C_{i-1}\right), & \text{otherwise}, \end{cases} \tag{5}$$

where $C_i(t)$ is the numerical approximation to the function $c(r_i, t)$ at the spatial grid point $r_i = i\Delta r$ for $i = 0, 1, \ldots, M$ with time as a continuous variable. We refer to this scheme (5) as Scheme 0.

Finite difference schemes for the diffusion PDE (1) in rectangular coordinates with variable diffusivity are available. One such method (Savovic and Djordjevich, 2012) requires that the spatial derivative of the diffusivity be evaluated analytically and explicitly as a function of position and time, which is not possible for diffusivity dependent on concentration or implicitly dependent on position and time. Other methods reviewed by (Mitchell and Griffiths, 1980) for discretization of the self-adjoint form, e.g., $\frac{\partial u}{\partial t} = \frac{\partial}{\partial x}\left(a\,(x,t)\,\frac{\partial u}{\partial x}\right)$ where the variable diffusivity remains inside the outer derivative, in rectangular coordinates are appropriate for extension to diffusion in spherical coordinates with variable diffusivity. Two finite difference schemes for variable diffusivity in spherical coordinates have been used in the literature for the cases of concentration-dependent diffusivity (Xanthopolous et al., 2012) and implicitly-defined, temporally- and spatially-dependent diffusivity (Ford Versypt, 2012). Neither of these methods has been analyzed previously for numerical accuracy or applicability to a wide range of cases of variable diffusivity.

Here, we present and compare two finite difference discretization schemes for numerically approximating the spatial derivatives of the diffusion equation (1) in spherical coordinates with variable diffusivity. The schemes are defined in Section 2, and the derivations for Schemes 0, 1, and 2 are included in Appendix A and Appendix B. In Section 3, five diffusivity cases are defined: (I) constant diffusivity α_0, (II) temporally-dependent diffusivity $\alpha(t)$, (III) spatially-dependent diffusivity $\alpha(r)$, (IV) concentration-dependent

diffusivity $\alpha(c(r, t))$, and (V) implicitly-defined, temporally- and spatially-dependent diffusivity $\alpha(f(r, t))$. Also in Section 3, analytical or semi-analytical solutions are presented for Cases I–IV. Case V can only be solved numerically and presents a rigorous test case for illustrating the performance of the finite difference schemes. In Section 4, Schemes 1 and 2 and the method of lines are applied to numerically solve each diffusivity case, and the errors between the numerical and analytical or semi-analytical solutions are analyzed. This analysis provides support for recommending Scheme 1 as the preferred finite difference method for numerically solving the diffusion equation in spheres with variable diffusivity.

2. Finite difference discretization schemes

The two finite difference schemes presented here employ the central difference operator (see Appendix A.1) to approximate spatial derivatives centered about the grid point r_i using two adjacent neighboring grid points. The limit of the diffusion PDE (1) at $r = 0$ is used to derive the $i = 0$ boundary condition for Schemes 1 and 2 as well as for Scheme 0 (see Appendix B).

By distributing the outer derivative to the inner terms, the terms in the diffusion PDE (1) can be expanded to yield the equivalent alternative forms

$$\frac{\partial c}{\partial t}=\frac{2\alpha}{r}\frac{\partial c}{\partial r}+\frac{\partial}{\partial r}\left(\alpha\frac{\partial c}{\partial r}\right) \quad (6)$$

and

$$\frac{\partial c}{\partial t}=\frac{2\alpha}{r}\frac{\partial c}{\partial r}+\frac{\partial \alpha}{\partial r}\frac{\partial c}{\partial r}+\alpha\frac{\partial^2 c}{\partial r^2}. \quad (7)$$

Schemes 1 and 2 differ by which terms remain within the outer spatial derivative of the diffusion PDE (1) after the outer derivative has been distributed when the central finite differences are applied. In (6), the diffusivity and the first spatial derivative of the concentration remain inside the outer derivative. Both Scheme 0 (see Appendix A.1) and Scheme 1 (see Appendix A.2) are derived by approximating the spatial derivatives in (6) with central finite differences in the interior of the spherical domain for $0 < r < 1$. In (7), the outer spatial derivative in the diffusion PDE (1) has been fully distributed to all the inner terms. Scheme 2 is derived by approximating the spatial derivatives in (7) with central finite differences in the interior of the spherical domain for $0 < r < 1$ (see Appendix A.3). The numerical approximations to the functions $c(r_i, t)$ and $\alpha(r_i, t)$ at the spatial grid point $r_i = i\Delta r$ with time as a continuous variable are denoted as $C_i(t)$ and $A_i(t)$, respectively.

Scheme 1 considers $\alpha(r, t)$ by preserving the self-adjoint form of the second term in the PDE (6) and by approximating the intermediate grid points with the average value at the adjacent grid points:

$$\frac{dC_i}{dt}=\begin{cases}\frac{6A_0(C_1-C_0)}{\Delta r^2}, & \text{if } i=0;\\ 0, & \text{if } i=M;\\ \frac{A_i}{2i\Delta r^2}\left((i+2)C_{i+1}-2iC_i+(i-2)C_{i-1}\right)+\frac{A_{i+1}}{2\Delta r^2}\left(C_{i+1}-C_i\right)+\frac{A_{i-1}}{2\Delta r^2}\left(C_{i-1}-C_i\right), & \text{otherwise.}\end{cases} \quad (8)$$

Scheme 1 has been used to treat drug-loaded, biograding polymeric systems with implicily-defined, temporally- and spatially-dependent diffusivity to predict the cumulative amount of drug released over time (Ford Versypt, 2012).

Scheme 2 considers $\alpha(r, t)$ by adding a contribution from the spatial derivative of to Scheme 0:

$$\frac{dC_i}{dt} = \begin{cases} \frac{6A_0}{\Delta r^2}\left(C_1 - C_0\right), & \text{if } i=0; \\ 0, & \text{if } i=M; \\ \frac{A_i}{i\Delta r^2}\left((i+1)\,C_{i+1} - 2iC_i + (i-1)\,C_{i-1}\right) + \frac{A_{i+1}}{4\Delta r^2}\left(C_{i+1} - C_{i-1}\right) + \frac{A_{i-1}}{4\Delta r^2}\left(C_{i-1} - C_{i+1}\right), & \text{otherwise.} \end{cases} \quad (9)$$

Scheme 2 has been used for food drying systems to estimate the coefficients in a concentration-dependent diffusivity functional form and to predict the moisture content within a spherical tomato over time (Xanthopolous et al., 2012).

3. Diffusivity dependences

Five cases for the functional form of the diffusivity, α, are described in the following subsections. These cases are used as benchmarks for assessing the performance of Schemes 1 and 2 in Section 4. Analytical solutions for Cases I and II and semi-analytical solutions for Cases III and IV are presented for validating the schemes in Section 4.

3.1. Case I: Constant diffusivity

The diffusion PDE (1) with constant diffusivity ($\alpha(r, t) = \alpha_0$), the initial condition (2), and the boundary conditions (3) and (4) can be transformed by defining a new variable $u = cr$, which yields a linearized PDE that matches the diffusion equation in rectangular coordinates (see (Crank, 1975) for derivation). Substituting the transformed variable into the analytical solution for the linearized PDE and rearranging gives

$$c\left(0,t\right) = -2\sum_{n=1}^{\infty}(-1)^n \exp\left(-n^2\pi^2\alpha_0 t\right) \quad (10)$$

for $r = 0$ and

$$c\left(r,t\right) = \frac{-2}{\pi r}\sum_{n=1}^{\infty}\frac{(-1)^n}{n}\exp\left(-n^2\pi^2\alpha_0 t\right)\sin\left(n\pi r\right) \quad (11)$$

for $0 < r < 1$. The parameters $\alpha_0 = D/R^2$, $D = 1.5 \times 10^{-13}$ cm^2/s, and $R = 25$ μm are used here, and the summations are truncated at $n = 300$ (due to the n^2 terms in the exponential in (10) and (11), the convergence is very fast for any fixed $t > 0$).

3.2. Case II: Temporally-dependent diffusivity

If the diffusivity depends on time and not on spatial position, then $\alpha(r, t) = \alpha(t)$: The diffusion PDE (1) with diffusivity that depends on time and not on spatial position ($\alpha(r, t) = \alpha(t)$) can be transformed by defining a new time variable $\int_0^t \alpha\left(t'\right)/\alpha_0 dt'$, which yields a PDE with constant coefficients (Crank, 1975):

$$\frac{\partial c}{\partial T}=\frac{1}{r^2}\frac{\partial}{\partial r}\left(r^2\alpha_0\frac{\partial c}{\partial r}\right). \quad (12)$$

The solution to (12) is given by (10) and (11) with T substituted for t. For the comparisons of numerical algorithms, $\alpha(t)$ was specified as a piecewise function with a constant value before some time τ and temporally-dependent exponential growth after time τ,

$$\alpha(t)=\begin{cases}\alpha_0, & \text{if } t<\tau;\\ \alpha_0\exp(k(t-\tau)), & \text{otherwise.}\end{cases} \quad (13)$$

Evaluating T for this $\alpha(t)$ gives

$$T=\begin{cases}t, & \text{if } \quad t<\tau;\\ \frac{1}{k}(\exp(k(t-\tau))-1+k\tau), & \text{otherwise.}\end{cases} \quad (14)$$

The parameters $\alpha_0 = D/R^2$, $D = 1.5 \times 10^{-13}$ cm^2/s, $R = 25$ μm, $\alpha_0\tau = 0.1175$, and $k = 10/\tau$ are used here. As in Case I, the summations are truncated at $n = 300$.

3.3. Case III: Spatially-dependent diffusivity

The diffusion PDE (1) for diffusivity that depends on spatial position and not time ($\alpha(r, t) = \alpha(r)$) can be transformed by defining a new variable $w(r) = -r^2\alpha(r)\frac{\partial c}{\partial r}$ that includes all the terms inside the outer derivative of the diffusion PDE (1), which yields the conservation form of the PDE (Mitchell and Griffiths, 1980):

$$\frac{\partial c}{\partial t}+\frac{1}{r^2}\frac{\partial w}{\partial r}=0. \quad (15)$$

For certain functions of $\alpha(r)$, a semi-analytical solution to (15) is obtained by numerically approximating the first spatial derivative of w with the second-order accurate, central finite difference scheme for $i = 1, 2, \ldots, M–1$ and $t > 0$ (Mitchell and Griffiths, 1980):

$$\frac{dC_i}{dt}=\frac{1}{i^2\Delta r^2}\frac{W_{i-1/2}-W_{i+1/2}}{\Delta r}, \quad (16)$$

where

$$W_{i-1/2}\int_{(i-1)\Delta r}^{i\Delta r}\frac{dr}{r^2\alpha(r)}=C_{i-1}-C_i \quad (17)$$

and

$$W_{i+1/2}\int_{i\Delta r}^{(i+1)\Delta r}\frac{dr}{r^2\alpha(r)}=C_i-C_{i+1}, \quad (18)$$

assuming that $w = W_{i-1/2}$ over the interval $[(i-1)\Delta r, i\Delta r]$ and $w = W_{i+1/2}$ over the interval $[i\Delta r, (i+1)\Delta r]$.

For the comparisons of algorithms, $\alpha(r) = \alpha_0 r^2$ was specified, which enabled the analytical evaluation of the integrals in (17) and (18). After integrating, applying the boundary conditions, and simplifying, (16) becomes

$$\frac{dC_i}{dt} = \begin{cases} 0, & \text{if} \quad i=0; \\ 0, & \text{if} \quad i=M; \\ \frac{3\alpha_0 i(C_{i+1}-C_i)}{1-\left(\frac{i}{i+1}\right)^3} - \frac{3\alpha_0 i(C_i-C_{i-1})}{\left(\frac{i}{i-1}\right)^3-1}, & \text{otherwise.} \end{cases} \quad (19)$$

The numerical scheme (19) can be solved with fine resolution ($\Delta r = 10^{-3}$, $M = 1000$) and is used as the semi-analytical solution for Case III. The parameters $\alpha_0 = D/R^2$, $D = 1.5 \times 10^{-13}$ cm^2/s, and $R = 25$ μm are used here.

3.4. Case IV: Concentration-dependent diffusivity

The diffusion PDE (1) for diffusivity that depends on the concentration explicitly and the spatial position and time implicitly ($\alpha(r, t) = \alpha(c(r, t))$) can be transformed by defining a new variable $S = \int_0^c \alpha(c)/\alpha_0 dc$, which yields a simplified PDE with a variable coefficient outside the spatial derivative term (Hsu, 1983):

$$\frac{\partial S}{\partial t} = \frac{\alpha(S)}{r^2}\frac{\partial}{\partial r}\left(r^2\frac{\partial S}{\partial r}\right). \quad (20)$$

We specified $\alpha(c) = \alpha_0 \exp(k - kc(r, t))$, which enabled the analytical evaluation of S. Solving the integral in the definition of S yields

$$S = \frac{1-\exp(k(1-c))}{k} = \frac{1-\alpha/\alpha_0}{k} \quad (21)$$

and

$$\alpha(S) = \alpha_0(1-kS). \quad (22)$$

The initial condition is $S(r, 0) = 0$, and the boundary conditions are $\frac{\partial S(0,t)}{\partial r} = 0$ and $S(1, t) = (1 - \exp(k))/k$. The PDE for S (20) can be solved numerically by approximating the spatial derivatives of S with second-order accuracy using Scheme 0 multiplied by the prefactor $\alpha(S)$ given by (22) evaluated at $S(r_i, t) \approx S_i(t)$ (Mitchell and Griffiths, 1980; Hsu, 1983):

$$\frac{dS_i}{dt} = \begin{cases} \frac{6\alpha_0(1-kS_0)}{\Delta r^2}(S_1 - S_0), & \text{if} \quad i=0; \\ 0, & \text{if} \quad i=M; \\ \frac{\alpha_0(1-kS_i)}{i\Delta r^2}((i+1)S_{i+1} - 2iS_i + (i-1)S_{i-1}), & \text{otherwise.} \end{cases} \quad (23)$$

The numerical scheme (23) can be solved with fine resolution ($\Delta r = 10^{-3}$, $M = 1000$). The solution for S_i is substituted into (21) and solved for C_i, which is used as the semi-analytical solution for Case IV. The parameters $\alpha_0 = D/R^2$, $D = 1.5 \times 10^{-13}$ cm^2/s, $R = 25$ μm, and $k = 1$ are used here.

3.5. Case V: Implicitly-defined, temporally- and spatially-dependent diffusivity

In the general case of variable diffusivity, the diffusivity depends on the spatial position and time. This dependence may not be explicitly defined. Instead, the diffusivity may be defined as a function of another variable that may have an analytical or numerical solution as a function of position and time. Here, we consider $\alpha(r, t) = \alpha(f(r, t))$ where $f(r, t)$ is a series of functions that describe the diffusion through the nonporous polymer bulk and through the growing pores of a chemically-degrading sphere used in drug delivery applications (Ford Versypt, 2012).

The effective diffusivity for a drug diffusing out of a polymer microsphere that chemically degrades uniformly throughout the polymer bulk subject to a catalyst that may accumulate or diffuse is defined as (Ford Versypt, 2012)

$$\alpha(\lambda) = (D_b + D_\infty H(\lambda)/\tau)/R^2, \quad (24)$$

where D_b is the diffusivity in the polymer bulk, D_∞ is the diffusivity in aqueous solution at infinite dilution at the operating temperature of 310 K, and τ is the average tortuosity of the pores (see Table 1 for values). The hindrance factor, $H(\lambda)$, accounting for porosity and hydrodynamic restrictions on the diffusion of the solute in fine, liquid-filled pores is (Deen, 1987; Dechadilok and Deen, 2006)

$$H(\lambda) = \begin{cases} \frac{6\pi(1-\lambda)^2}{K(\lambda)}, & \text{if} \quad 0 \le \lambda \le 1; \\ 0, & \text{otherwise}, \end{cases} \quad (25)$$

where $\lambda = R_d/R_p(r, t)$, R_d and $R_p(r, t)$ are the radii of the diffusing drug species and the growing pore, respectively, and the hydrodynamic coefficient $K(\lambda)$ is given by (Bungay and Brenner, 1973)

$$K(\lambda) = \frac{9\pi^2\sqrt{2}}{4}(1-\lambda)^{-5/2}\left(1 + \sum_{j=1}^{2} a_j (1-\lambda)^j\right) + \sum_{j=0}^{4} a_{j+3}\lambda^j, \quad (26)$$

with the coefficients a_j: $a_1 = -73/60$, $a_2 = 77293/50400$, $a_3 = -22.5083$, $a_4 = -5.6117$, $a_5 = -0.3363$, $a_6 = -1.216$, and $a_7 = 1.647$.

Analytical solutions for the concentration of the catalyst were used to approximate the average pore radius, $R_p(r, t)$, as a function of time and position within a degrading sphere with growing pores (Ford Versypt, 2012). For the case of $\Phi_a = m\pi$ where m is an integer,

$$R_p(0, t) = R_{p0} - 2\beta k(-1)^m t + \sum_{\substack{n=1 \\ n \neq m}}^{\infty} \frac{2\beta\Phi_a^2(-1)^n}{n^2\pi^2 - \Phi_a^2} \times \left(\exp\left(-\left(n^2\pi^2 - \Phi_a^2\right)\alpha_a t\right) - 1\right), \quad (27)$$

and for $0 < r < 1$

$$R_p(r,t) = R_{p0} - \frac{2\beta k(-1)^m t \sin(m\pi r)}{m\pi r} \sum_{\substack{n=1 \\ n\neq m}}^{\infty} \frac{2\beta\Phi_a^2(-1)^n \sin(n\pi r)}{n\pi r\left(n^2\pi^2 - \Phi_a^2\right)} \times \left(\exp\left(-\left(n^2\pi^2 - \Phi_a^2\right)\alpha_a t\right) - 1\right), \quad (28)$$

where R_{p0} is the initial pore radius, β is a parameter that includes the effects of the molecular weight and solubility of the polymer, k is the rate constant for the degradation reaction, α_a is the diffusivity of the acidic catalyst in the polymer, and $\Phi_a = \sqrt{k/\alpha_a}$ (see Table 1 for values).

If the initial porosity of the sphere, R_{p0}, is less than the drug molecule radius, R_d, then $H(\lambda)$ has an initial value of 0. With $H = 0$ at $t = 0$, the diffusion of the drug begins with a constant diffusivity of D_b as in Case I. Later, a spatial gradient in the average pore size, R_p, develops yielding different times when $H(\lambda)$ becomes nonzero at each position. As the porosity continues to grow, the diffusivity varies as a function of position and time. To predict the amount of the drug released from the sphere over time, it is important to have a numerical method that can treat the diffusivity defined in (24)–(28) for Case V.

4. Numerical and analytical results and discussion

Both numerical discretization schemes (Schemes 1 and 2) are used to reduce the diffusion PDE (1) to a system of ODEs that are solved using the RADAU5 implicit ODE solver (Hairer and Wanner, 1996) with $M = 100$ spatial grid resolution and 100 minimum time steps per time interval (e.g., $0 < t \leq 1/\alpha_0$). The solver utilizes adaptive time-stepping and typically uses many more than the minimum number of time steps, as needed to maintain the tolerance of 10^{-6} in the algorithm. The numerical solutions using both schemes are compared to the analytical or semi-analytical solution for each of the following four cases for the functional form of defined in Section 3: (I) α_0, (II) $\alpha(t)$, (III) $\alpha(r)$, and (IV) $\alpha(c(r, t))$. Case V, $\alpha(f(r, t))$, for which no analytical solution is available, is used to compare solutions for the most general type of expression for the diffusivity. In Section 4.1, the errors between the numerical and analytical or semi-analytical solutions are analyzed for Cases I–IV. The concentration profiles for Cases I–V obtained by the analytical or semi-analytical solutions and the numerical solutions with Schemes 1 and 2 are presented in Section 4.2. In Section 4.3, the cumulative fraction of the diffusing species released as a function of time is compared for diffusivity Cases I–V.

4.1. Error analysis

The 2-norm of the error between the grid function numerical solution, C_i^j, and the true solution, $c(r_i, t_j)$, is used to assess the error between the numerical and analytical or semi-analytical solutions, (LeVeque, 2007)

$$||e||_2 = \left(\frac{1}{MN} \sum_{i=0}^{M-1} \sum_{j=1}^{N} |e_{i,j}|^2 \right)^{1/2} = \left(\frac{1}{MN} \sum_{i=0}^{M-1} \sum_{j=1}^{N} \left(c\left(r_i, t_j\right) - C_i^j \right)^2 \right)^{1/2} \quad (29)$$

where the numerical approximation, C_i^j, is a grid function on the grid points $r_i = i\Delta r$ for $i = 0, 1, \ldots, M$ and $t_j = j\Delta t$ for $j = 0, 1, \ldots, N$. The boundary condition at $r = 1$ and the initial condition at $t = 0$ are not included in this error estimate, because these values are specified and not approximated. The error estimate (29) is analogous to the root-mean-square error defined as the square root of the mean of the errors between measured values and values predicted by a model.

When using an ODE solver with adaptive time stepping, Δt is not uniform. However, the maximum t is specified to the solver, so (29) may be used to determine an upper bound of the error estimate. This error was estimated for Cases I-IV by comparing the numerical solutions using Schemes 1 and 2 to the analytical or semi-analytical solution for each case (Table 2). As a benchmark, the error was estimated for the numerical solution using Scheme 0 with a_0 in the scheme definition (5) replaced by $a(r_i, t)$ for each case.

With constant or temporally-dependent diffusivity where the diffusivity can be factored out of the outer derivative term in the PDE (1), Schemes 1 and 2 collapse to Scheme 0 with a_0 replaced by $a(t)$. Thus the error is the same for all three schemes in Cases I and II.

Scheme 0 does not account for the impact of the spatial gradient in the diffusivity in Cases III and IV, therefore the error is large for Scheme 0 in these cases. Scheme 0 should not be used for treating diffusivity with spatial dependence.

In Cases III and IV, the numerical error for Scheme 1 is smaller than for Scheme 2. This result, along with the equivalent performance between the schemes for Cases I and II, suggests that the spatial derivative of the diffusivity was approximated more accurately by Scheme 1 than by Scheme 2.

4.2. Concentration profiles

The concentration profiles obtained by Schemes 1 and 2 in Cases I–IV are indistinguishable (Figures 1, 2, 3, 4), which is consistent with the error estimates (Table 2). The errors estimated for Schemes 1 and 2 in Cases I and II are equivalent and only differ to a small extent with the same number of significant figures in Cases III and IV (4 and 5, respectively). In contrast, the concentration profiles for Case V obtained by Scheme 1 (Figures 5(a) and 6) differ strikingly from those obtained by Scheme 2 (Figure 6), which diverge after the diffusivity becomes transient and develops a spatial gradient. Below is a more detailed discussion of the simulation comparisons.

4.2.1. Case I—The concentration profiles (Figure 1) for Case I ($a = a_0$) obtained by both numerical schemes are in good agreement with the analytical solution defined by (10) and (11). The species becomes depleted in the sphere by $t = 1/a_0$.

4.2.2. Case II—The concentration profiles (Figure 2) for Case II ($a = a_0$ for $t \leq \tau$ and $a = a_0 \exp(k(t - \tau))$ for $t > \tau$) obtained by both numerical schemes are in good agreement with the analytical solution defined by (10) and (11) with T substituted for t and defined by (14). The profiles before $t = \tau = 0.1175/a_0$ are the same as for constant diffusivity (Case I). For $t > \tau$, the diffusion is accelerated, and the species becomes depleted in the sphere by $t = 0.2/a_0$.

4.2.3. Case III—The concentration profiles (Figure 3) for Case III ($a = a_0 r^2$) obtained by both numerical schemes are in good agreement with the semi-analytical solution defined by (19). With the diffusivity at $r = 0$ having a value of 0, the concentration at the center of the sphere remains constant at its initial value of 1. This results in concentration profiles that do not uniformly decay to zero. The average diffusivity within the sphere is less than a_0, so the diffusion is slower than for the constant diffusivity results in Case I.

4.2.4. Case IV—The concentration profiles (Figure 4) for Case IV ($a = a_0 \exp(k - kc)$) obtained by both numerical schemes are in good agreement with the semi-analytical solution defined by (23) with S_i substituted into (21) and solved for C_i. The diffusivity grows with decreasing concentration, so the diffusion accelerates and proceeds faster than for the constant diffusivity in Case I. The species becomes depleted in the sphere by $t = 0.28/a_0$.

4.2.5. Case V—The concentration profiles (Figure 5) for Case V ($a = a(f(r, t))$ defined implicitly by (24)–(28)) have no analytical or semi-analytical solution. This case is presented to illustrate the difference between the performance of Schemes 1 and 2 with the implicitly-defined, temporally- and spatially-dependent diffusivity.

Before $t = 0.1175/a_0$, the diffusivity is constant, and the concentration profiles obtained by both numerical schemes are in agreement. After the diffusivity begins to vary, the diffusivity at the center of the sphere is larger than the diffusivity at the surface. Scheme 1 shows a wave of mass diffusing towards the surface develops over time (e.g., the right-hand edges of the curves at times $t = 0.12/a_0$, $t = 0.135/a_0$, and $t = 0.15/a_0$ in Figure 5(a)). This behavior has a physical explanation. Consider the analogy of water draining from a tank. If the water from the edges of the tank is accelerated towards a drain at the center without the ability to flow backwards, water accumulates temporarily near the drain until the water can flow out of the tank. In Case V, the diffusing species can diffuse faster away from the center of the sphere than it can be transported across the surface of the sphere. Eventually, all of the species diffuses through the surface, and the species becomes depleted in the sphere by $t = 0.2/a_0$.

After the diffusivity becomes transient at $t = 0.1175/a_0$ and develops a spatial gradient, Scheme 2 diverges from Scheme 1 (compare the curves for $t = 0.135/a_0$ and $t = 0.15/a_0$ in Figures 5(a) and 5(b) and see Figure 6). The divergence rapidly becomes increasingly severe as time progresses (e.g., for Scheme 2 the numerical approximation of the dimensionless concentration at $t = 0.1575/a_0$ is $C_0(t) = 6.5 \times 10^{13}$, not shown). The spatial derivative term of the diffusivity in Scheme 2 artificially allows flux of the diffusing species into the sphere (against the concentration gradient) and does not conserve the species (Figure 5(b)).

Scheme 2 has poor numerically accuracy in simulating the concentration profiles in Case V. The numerical instabilities and inaccuracies of Scheme 2 can be induced by the central difference discretization of the second term in (7), $\frac{\partial \alpha}{\partial r}\frac{\partial c}{\partial r}$, which is a hyperbolic, convection term for the concentration with a varying coeffcient in front. This term causes problems when $\frac{\partial \alpha}{\partial r}$ is large enough to make the overall second term in (7) larger than the diffusive third term in (7), $\alpha\frac{\partial^2 c}{\partial r^2}$. For $t > 0.12/a_0$, $\frac{\partial \alpha}{\partial r}$ is large (Figure 7), and this steep gradient contributes to the development of the numerical instabilities (Figure 5(b)). It is well-known that central differences lead to aphysical oscillations for convection-diffusion equations when the convective term dominates (LeVeque, 2007). The $\frac{\partial \alpha}{\partial r}\frac{\partial c}{\partial r}$ term could be implemented by first-order upwinding but that would lower the accuracy. Scheme 1 uses central differences with second-order accuracy in space on the combined diffusive term $\frac{\partial}{\partial r}\left(\alpha\frac{\partial c}{\partial r}\right)$ in (6), which avoids creating the separate convective term $\frac{\partial \alpha}{\partial r}\frac{\partial c}{\partial r}$ that causes problems in Scheme 2. Diffusive terms are well handled by second-order central differences, so Scheme 1 provides much higher numerical accuracy for problems where $\frac{\partial \alpha}{\partial r}$ is large.

4.3. Cumulative fraction released

The cumulative normalized fraction of diffusing species released as a function of time, $Q(t)$, is the ratio of the cumulative amount released as a function of time to the cumulative amount released in the limit as $t \to \infty$ (Ford Versypt, 2012):

$$Q(t) = \frac{\int_0^1 (c(r,0) - c(r,t))\, r^2 dr}{\int_0^1 (c(r,0) - c(1-t))\, r^2 dr}. \quad (30)$$

The calculation of $Q(t)$ uses the initial distribution $c(r, 0) = 1$, the constant surface concentration $c(1, t) = 0$, the discrete values of r along the radius, and the values of $c(r_i, t)$ determined from the analytical or numerical solution to the PDE (1). The numerator and denominator of (30) can be integrated numerically by the adaptive Simpson quadrature implemented by the function “quad” in MATLAB. The profiles for the cumulative fraction released are compared for Cases I–V (Figure 8).

The cumulative fraction released in Case I is in good agreement with the analytical expression for the quantity in the case of constant diffusivity (Crank, 1975). In Case II, the diffusion is accelerated resulting in the cumulative fraction released reaching its maximum of 1 earlier than with constant diffusivity (Case I). In Case III, the diffusion is slower than with constant diffusivity (Case I) resulting in a profile for the cumulative fraction released that takes longer to reach its maximum than the profile for Case I. In Case IV, the diffusion is accelerated as the concentration decreases yielding a profile for the cumulative fraction released that reaches its maximum much faster than the profile for Case I.

For Cases II and V, the diffusivities become transient at the same time point ($t = 0.1175/\alpha_0$). Using Scheme 1 for Case V, the profile for the cumulative fraction released rises rapidly, although not as sharply as in Case II, and reaches its maximum faster than the profile for Case I. Using Scheme 2 for Case V (not shown), the profile for the cumulative fraction released decreases with time as the concentration profiles diverge. Eventually, the profile becomes negative indicating that Scheme 2 is non-conservative and artificially allows diffusion into the sphere from the medium due to the gradient in the diffusivity.

5. Conclusions

Both Schemes 1 and 2 use central differences that are second-order accurate in Δr for approximating the spatial derivatives of the diffusion equation (1). Scheme 1 is consistent with the finite difference methods described in (Mitchell and Griffiths, 1980) applied to the self-adjoint diffusion PDE in rectangular coordinates. It is generally recommended to approximate derivatives in the self-adjoint form (Mitchell and Griffiths, 1980; Morton and Mayers, 2005) as in Scheme 1. Section 4 reported two main findings: (1) Scheme 1 had higher accuracy than Scheme 2 for Cases III–IV, and (2) Scheme 1 gives physically realistic, numerically stable concentration profiles and cumulative fraction released profiles for Case V, while Scheme 2 numerically diverges and does not conserve the amount of species in the sphere. Based upon the results of our analysis, the second-order accuracy of the discretization scheme, and the advice for discretizing the self-adjoint form of the diffusion PDE, i.e., (6), we recommend the adoption of the finite difference discretization scheme referred to here as Scheme 1 to numerically approximate the spatial derivatives of the diffusion equation for any case of variable diffusivity and especially those cases where the diffusivity is a function of position (such as Cases III-V).

Appendix A. Derivation of spatial discretization schemes in the range 0 < r < 1

The interior portion of the spatial domain in the range $0 < r < 1$ discretized by Δr into M uniform discretizations is considered first. The central difference operator notation of (Morton and Mayers, 2005) is adopted where the operator δ_{kr} centered in the r-dimension at position r_i over an interval of $k\Delta r$ applied to $c(r_i, t)$ is

$$\begin{aligned}\delta_{kr} c\left(r_i, t\right) &= c\left(r_i + k\Delta r/2, t\right) - c\left(r_i - k\Delta r/2, t\right) \\ &\approx C_{i+k/2}\left(t\right) - C_{i-k/2}\left(t\right),\end{aligned} \tag{A.1}$$

where $C_i(t) \approx c(r_i, t)$.

Appendix A.1. Scheme 0

Scheme 0 is the the common finite difference discretization scheme for diffusion in spherical geometry with constant diffusivity (Crank, 1975; Carslaw and Jaeger, 1986; Ozisik, 1993; Morton and Mayers, 2005). The scheme is derived by applying the central finite difference approximation to the spatial derivatives in (6) with $\alpha(r, t) = \alpha_0$ at $(r_i, t) = (i\Delta r, t)$ for $i = 1, 2, \ldots, M - 1$ and $t > 0$:

$$\begin{aligned}&\frac{\alpha_0}{i\Delta r^2}\delta_{2r}c\left(r_i,t\right)+\frac{\alpha_0}{\Delta r^2}\delta_r\left(\delta_r c\left(r_i,t\right)\right)\\&=\frac{\alpha_0}{i\Delta r^2}\delta_{2r}c\left(r_i,t\right)+\frac{\alpha_0}{\Delta r^2}\delta_r\left(c\left(r_i+\Delta r/2,t\right)-c\left(r_i-\Delta r/2,t\right)\right)\\&\approx\frac{\alpha_0}{i\Delta r^2}\left(C_{i+1}-C_{i-1}\right)+\frac{\alpha_0}{\Delta r^2}\left(C_{i+1}-2C_i+C_{i-1}\right)\\&\approx\frac{\alpha_0}{i\Delta r^2}\left(\left(i+1\right)C_{i+1}-2iC_i+\left(i-1\right)C_{i-1}\right).\end{aligned}\tag{A.2}$$

Substituting the approximation for the spatial derivatives (A.2) into the PDE (6) and rearranging gives Scheme 0 in the ODE form used for the method of lines for $i = 1, 2, \ldots, M - 1$ and $t > 0$:

$$\frac{dC_i}{dt}=\frac{\alpha_0}{i\Delta r^2}\left(\left(i+1\right)C_{i+1}-2iC_i+\left(i-1\right)C_{i-1}\right).\tag{A.3}$$

Appendix A.2. Scheme 1

Scheme 1 is derived by applying the central finite difference approximation to the spatial derivatives in (6) at $(r_i, t) = (i\Delta r, t)$ for $i = 1, 2, \ldots, M - 1$ and $t > 0$:

$$\begin{aligned}&\frac{\alpha(r_i,t)}{i\Delta r^2}\delta_{2r}c\left(r_i,t\right)+\frac{1}{\Delta r^2}\delta_r\left(\alpha\left(r_i,t\right)\delta_r c\left(r_i,t\right)\right)\\&=\frac{\alpha(r_i,t)}{i\Delta r^2}\delta_{2r}c\left(r_i,t\right)+\frac{1}{\Delta r^2}\delta_r\left(\alpha\left(r_i,t\right)\left(c\left(r_i+\Delta r/2,t\right)-c\left(r_i-\Delta r/2,t\right)\right)\right)\\&\approx\frac{A_i}{i\Delta r^2}\left(C_{i+1}-C_{i-1}\right)+\frac{A_{i+1/2}}{\Delta r^2}\left(C_{i+1}-C_i\right)\Big)+\frac{A_{i-1/2}}{\Delta r^2}\left(C_{i-1}-C_i\right).\end{aligned}\tag{A.4}$$

In general for variable diffusivity, the values of the diffusivity at $r_i + \Delta r/2$ and $r_i - \Delta r/2$ are not available unless the function is approximated between grid points, which may be computationally expensive for complicated functional forms for $\alpha(r, t)$. Instead, the values of A at the intermediate grid points can be approximated using the known values at the adjacent grid points: $A_{i+1/2} \approx (A_{i+1} + A_i)/2$ and $A_{i-1/2} \approx (A_i + A_i - 1)/2$. Substituting these approximations and the approximation for the spatial derivatives (A.4) into the PDE (6) and rearranging gives Scheme 1 for $i = 1, 2, \ldots, M - 1$ and $t > 0$:

$$\frac{dC_i}{dt}=\frac{A_i\left(\left(i+2\right)C_{i+1}-2iC_i+\left(i-2\right)C_{i-1}\right)}{2i\Delta r^2}+\frac{A_{i+1}\left(C_{i+1}-C_i\right)}{2\Delta r^2}+\frac{A_{i-1}\left(C_{i-1}-C_i\right)}{2\Delta r^2}.\tag{A.5}$$

Scheme 1 preserves the self-adjoint form of the second term in the PDE (6).

Appendix A.3. Scheme 2

Scheme 2 is derived by applying the central finite difference approximation to the spatial derivatives in (7) at $(r_i, t) = (i\Delta r, t)$ for $i = 1, 2, \ldots, M - 1$ and $t > 0$:

$$\begin{aligned}&\frac{\alpha(r_i,t)}{i\Delta r^2}\delta_{2r}c\left(r_i,t\right)+\frac{1}{4\Delta r^2}\delta_{2r}\alpha\left(r_i,t\right)\delta_{2r}c\left(r_i,t\right)+\frac{\alpha(r_i,t)}{\Delta r^2}\delta_r\left(\delta_r c\left(r_i,t\right)\right)\\&=\frac{\alpha(r_i,t)}{i\Delta r^2}\delta_{2r}c\left(r_i,t\right)+\frac{1}{4\Delta r^2}\delta_{2r}\alpha\left(r_i,t\right)\delta_{2r}c\left(r_i,t\right)+\frac{\alpha(r_i,t)}{\Delta r^2}\delta_r\left(c\left(r_i+\Delta r/2,t\right)-c\left(r_i-\Delta r/2,t\right)\right)\\&\approx\frac{A_i}{i\Delta r^2}\left(C_{i+1}-C_{i-1}\right)+\frac{1}{4\Delta r^2}\left(A_{i+1}-A_{i-1}\right)\left(C_{i+1}-C_{i-1}\right)+\frac{A_i}{\Delta r^2}\left(C_{i+1}-2C_i+C_{i-1}\right).\end{aligned}\tag{A.6}$$

Substituting the approximation for the spatial derivatives (A.6) into the PDE (7) and rearranging gives Scheme 2 for $i = 1, 2, \ldots, M - 1$ and $t > 0$:

$$\frac{dC_i}{dt}=\frac{A_i\left((i+1)C_{i+1}-2iC_i+(i-1)C_{i-1}\right)}{i\Delta r^2}+\frac{\left(A_{i+1}-A_{i-1}\right)\left(C_{i+1}-C_{i-1}\right)}{4\Delta r^2}. \quad \text{(A.7)}$$

The first term of Scheme 2 resembles Scheme 0 except that α is evaluated at (r_i, t) and approximated by A_i rather than being constant with a value of α_0. The second term adds the contribution from the variable diffusivity.

Appendix B. Derivation of spatial discretization schemes at r = 0

The numerical schemes in Appendix A are valid for integers $i = 1, 2, \ldots, M - 1$. At the $r = 1$ boundary, the concentration is known explicitly by the constant surface boundary condition given by (4), so it is unnecessary to calculate updated values for $C_M(t) \approx c(1, t) = 0$. At the other boundary at the origin $r = 0$, the schemes given in (A.3), (A.5), and (A.7) each have a singularity at $i = 0$. Instead of adapting each scheme at the boundary, the singularity of the original PDE is treated before approximating the spatial derivatives.

In the limit as $r \to 0$, the right-hand side of (6) can be simplified as

$$\begin{aligned}\frac{\partial c(0,t)}{\partial t} &= \lim_{r\to 0}\left(\frac{2\alpha}{r}\frac{\partial c}{\partial r}+\frac{\partial}{\partial r}\left(\alpha\frac{\partial c}{\partial r}\right)\right)\\ &= 3\alpha\frac{\partial^2 c}{\partial r^2}\end{aligned} \quad \text{(B.1)}$$

after applying the boundary condition $\frac{\partial c(0,t)}{\partial r}=0$ and l'Hospital's Rule to resolve the indeterminate form of 0/0 in the first term.

The central difference approximation to the spatial derivatives in (B.1) is (Crank, 1975; Carslaw and Jaeger, 1986)

$$\begin{aligned}\frac{3\alpha}{\Delta r^2}\delta_r\left(\delta_r c(r_0,t)\right) &= \frac{3\alpha}{\Delta r^2}\delta_r\left(c\left(r_i+\Delta r/2,t\right)-c\left(r_i-\Delta r/2,t\right)\right)\\ &\approx \frac{3A_0}{\Delta r^2}\left(C_1-2C_0+C_{-1}\right).\end{aligned} \quad \text{(B.2)}$$

The boundary condition given by (3) enforces radial symmetry about the origin. The central difference approximation to the boundary condition is

$$\frac{\delta_{2r}c\left(r_{0,t}\right)}{2\Delta r}\approx\frac{C_1(t)-C_{-1}(t)}{2\Delta r}=0. \quad \text{(B.3)}$$

Solving for the concentration at the grid point outside the boundary gives $C_{-1}(t) = C_1(t)$.

Applying the approximation (B.2) to the simplified form of the PDE at $r = 0$ (B.1) and substituting $C_{-1} = C_1$, the equation for Schemes 0, 1, and 2 at $r = 0$ is

$$\frac{dC_0}{dt}=\frac{6A_0\left(C_1-C_0\right)}{\Delta r^2}. \quad \text{(B.4)}$$

References

Bungay PM, Brenner H. The motion of a closely-fitting sphere in a fluid-filled tube. Int J Multiphase Flow. 1973; 1(1):25–56.

Carslaw, HS.; Jaeger, JC. Conduction of Heat in Solids. 2nd ed.. Oxford University Press; New York: 1986.

Crank, J. The Mathematics of Diffusion. 2nd ed.. Oxford University Press; Oxford: 1975.

Dechadilok P, Deen WM. Hindrance factors for diffusion and convection in pores. Ind Eng Chem Res. 2006; 45(21):6953–9.

Deen WM. Hindered transport of large molecules in liquid-filled pores. AIChE J. 1987; 33(9):1409–25.

Ford, AN.; Pack, DW.; Braatz, RD. In: Pistikopoulos, EN.; Georgiadis, MC.; Kokossis, AC., editors. Multi-scale modeling of PLGA microparticle drug delivery systems; 21st European Symposium on Computer Aided Process Engineering: Part B; New York: Interscience. 2011; p. 1475-9.

Ford Versypt, AN. Ph.D. Dissertation. University of Illinois at Urbana-Champaign; Urbana, IL: 2012. Modeling of Controlled-Release Drug Delivery from Autocatalytically Degrading Polymer Microspheres.

Ford Versypt AN, Pack DW, Braatz RD. Mathematical modeling of drug delivery from autocatalytically degradable PLGA microspheres—A review. J Controlled Release. 2013; 165(1): 29–37.

Hairer, E.; Wanner, G. Solving Ordinary Differential Equations II: Sti and Differential-Algebraic Problems. 2nd ed.. Springer; New York: 1996.

Hsu KH. A diffusion model with a concentration-dependent diffusion coefficient for describing water movement in legumes during soaking. J Food Sci. 1983; 48(2):618–22.

LeVeque, RJ. Finite Difference Methods for Ordinary and Partial Differential Equations: Steady-State and Time-Dependent Problems. SIAM; Philadelphia: 2007.

Mitchell, AR.; Griffiths, DF. The Finite Difference Method in Partial Differential Equations. John Wiley & Sons; New York: 1980.

Morton, KW.; Mayers, DF. Numerical Solution of Partial Differential Equations. 2nd ed.. Cambridge University Press; New York: 2005.

Ozisik, MN. Heat Conduction. 2nd ed.. John Wiley & Sons; New York: 1993.

Petersen JS, Mack CA, Sturtevant JL, Byers JD, Miller DA. Nonconstant diffusion coefficients: Short description of modeling and comparison to experimental results. Proc SPIE. 1995; 2438:167–80.

Renganathan S, White RE. Semianalytical method of solution for solid phase diffusion in lithium ion battery electrodes: Variable diffusion coefficient. J Power Sources. 2011; 196(1):442–8.

Savovic S, Djordjevich A. Finite difference solution of the one-dimensional advection-diffusion equation with variable coefficients in semi-infinite media. Int J Heat Mass Transf. 2012; 23(9): 667–85.

Schiesser, WE. The Numerical Method of Lines: Integration of Partial Differential Equations. Academic Press; San Diego: 1991.

Schiesser, WE. Partial Differential Equation Analysis in Biomedical Engineering: Case Studies with MATLAB. Cambridge University Press; New York: 2013.

Tong CH, Lund DB. Effective moisture diffusivity in porous materials as a function of temperature and moisture content. Biotechnol Prog. 1990; 6(1):67–75.

Tsang T, Hammarstrom CA. Nonlinear diffusion in the solid phase. Ind Eng Chem Res. 1987; 26(4): 855–7.

Xanthopolous G, Yanniotis S, Boudouvis AG. Numerical simulation of variable water diffusivity during drying period of peeled and unpeeled tomato. J Food Sci. 2012; 77(10):E287–96. [PubMed: 22946755]

Zoppou C, Knight JH. Analytical solution of a spatially variable coefficient advection-diffusion equation in up to three dimensions. Appl Math Model. 1999; 23(9):667–85.

Highlights

- The diffusion equation in spherical coordinates with variable diffusivity is considered.
- Two finite difference discretization schemes are compared.
- The schemes are tested on five cases of the functional form for the variable diffusivity.
- A more accurate and numerically stable discretization scheme is recommended.

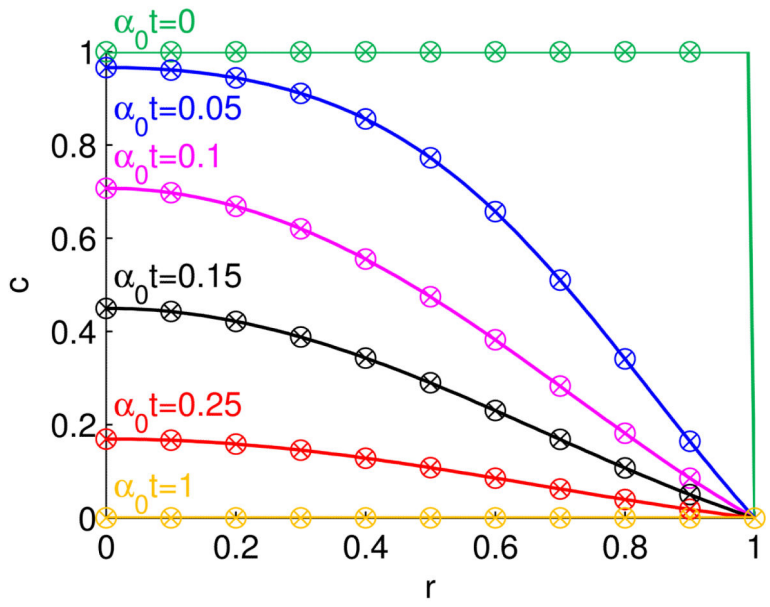

Figure 1.

Dimensionless concentration c as a function of dimensionless position r for Case I ($\alpha = \alpha_0$). Circles indicate Scheme 1 and ×'s indicate Scheme 2. The analytical solution is shown by solid curves. The numerical solutions used $M = 100$, but fewer grid points are shown for clarity. The parameters are $\alpha_0 = D/R^2$, $D = 1.5 \times 10^{-13}$ cm^2/s, and $R = 25$ μm.

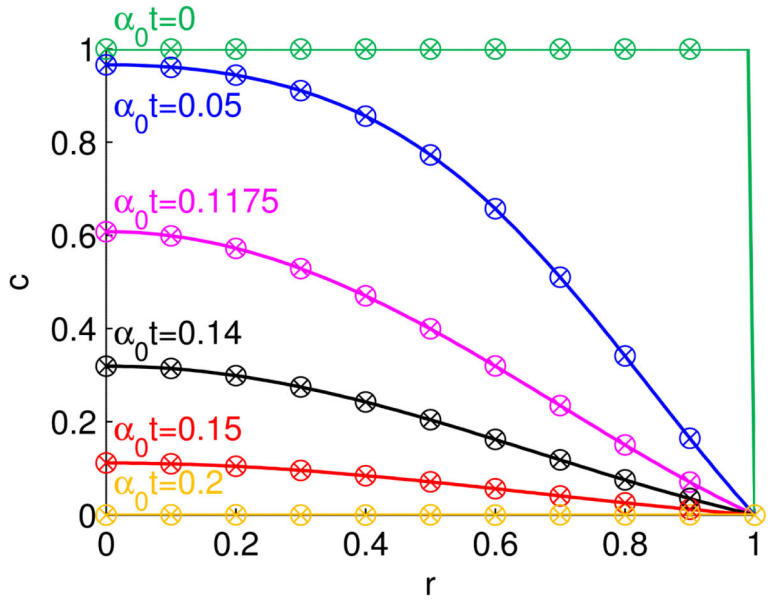

Figure 2.

Dimensionless concentration c as a function of dimensionless position r for Case II ($a = a_0$ for $t \geq \tau$ and $a = a_0 \exp(k(t - \tau))$ for $t > \tau$). Circles indicate Scheme 1 and ×'s indicate Scheme 2. The analytical solution is shown by solid curves at different times. The[notdef]numerical solutions used $M = 100$, but fewer grid points are shown for clarity. The parameters are $a_0 = aD/R^2$, $D = 1.5 \times 10^{-13}$ cm^2/s, $R = 25$ μm, $a_0\tau = 0.1175$, and $k = 10/\tau$.

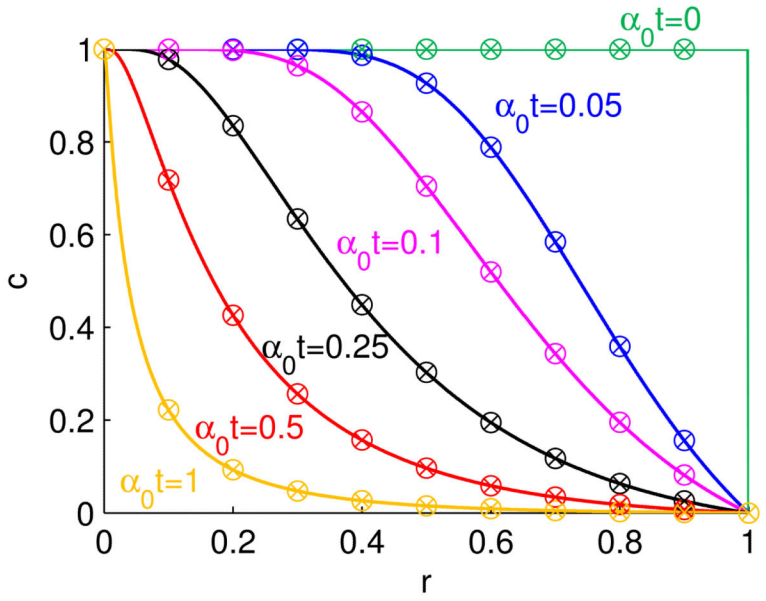

Figure 3.

Dimensionless concentration c as a function of dimensionless position r for Case III ($a = a_0 r^2$). Circles indicate Scheme 1 and ×'s indicate Scheme 2. The analytical solution is shown by solid curves at different times. The[notdef]numerical solutions used $M = 100$, but fewer grid points are shown for clarity. The parameters are $a_0 = D/R^2$, $D = 1.5 \times 10^{-13}$ cm^2/s, $R = 25$ μm.

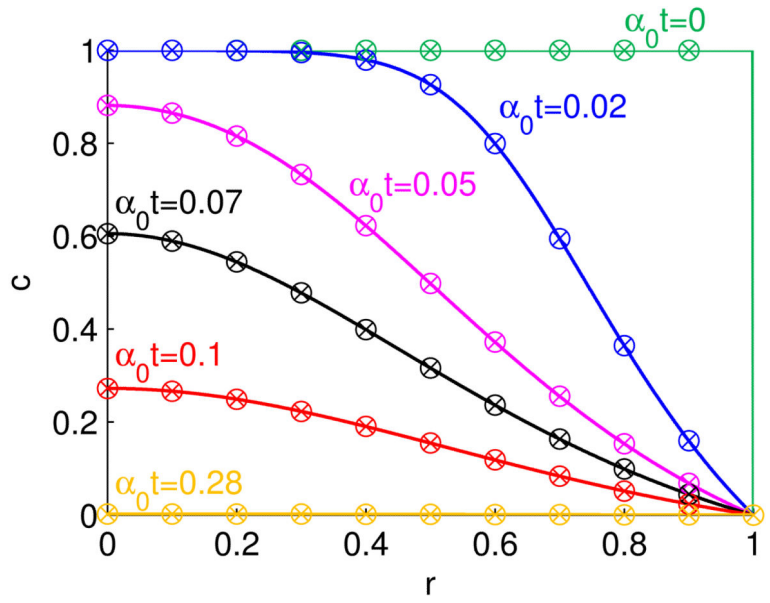

Figure 4.

Dimensionless concentration c as a function of dimensionless position r for Case IV ($a = a_0 \exp(k - kc)$). Circles indicate Scheme 1 and ×'s indicate Scheme 2. The analytical solution is shown by solid curves at different times. The[notdef]numerical solutions used $M = 100$, but fewer grid points are shown for clarity. The parameters are $a_0 = D/R^2$, $D = 1.5 \times 10^{-13}$ cm^2/s, $R = 25$ μm, and $k = 1$.

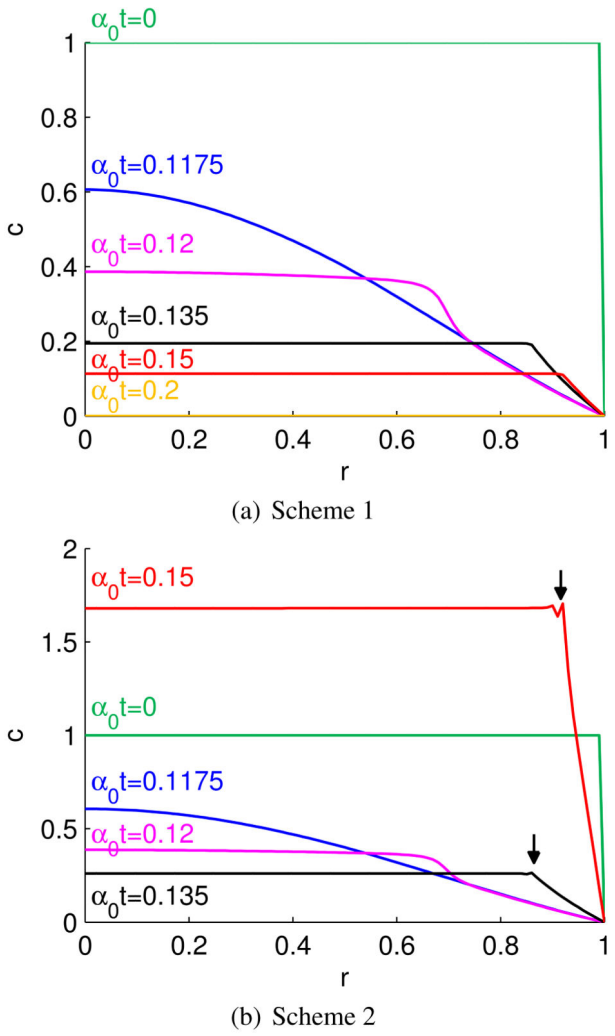

Figure 5.

Dimensionless concentration c as a function of dimensionless position r for Case V ($a = a(f(r, t))$). The numerical solutions are shown for $M = 100$ by solid curves at different times. In (b), arrows indicate the locations of numerical instabilities observed with Scheme 2. The parameters are given in Table 1, and $\alpha_0 = D_b/R^2 = 2.1 \times 10^{-3}$ days^{-1}.

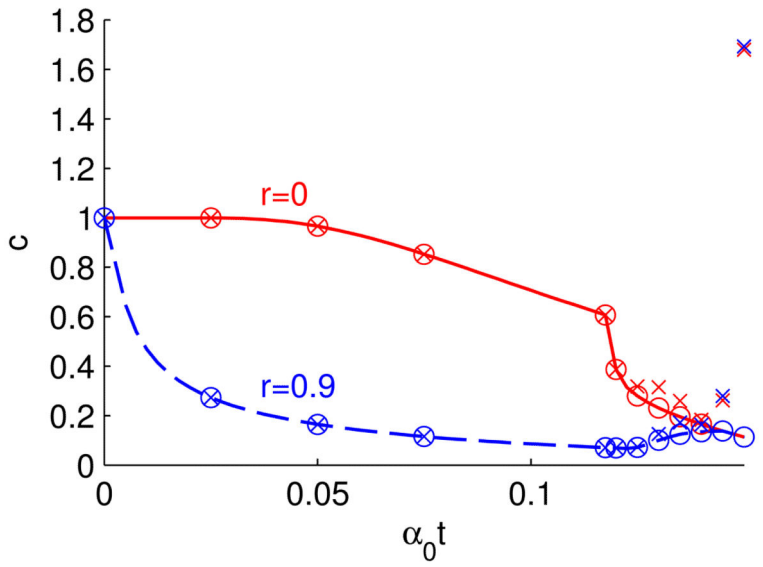

Figure 6.

Dimensionless concentration c as a function of dimensionless time $\alpha_0 t$ for Case V ($a = (f(r, t))$). The numerical solutions with Scheme 1 are shown by curves at two radial positions, with circles indicating Scheme 1 and ×'s indicating Scheme 2. The numerical solutions used $M = 100$, but fewer grid points are shown for clarity. The parameters are given in Table 1, and $\alpha_0 = D_b/R^2 = 2.1 \times 10^{-3}$ days^{-1}.

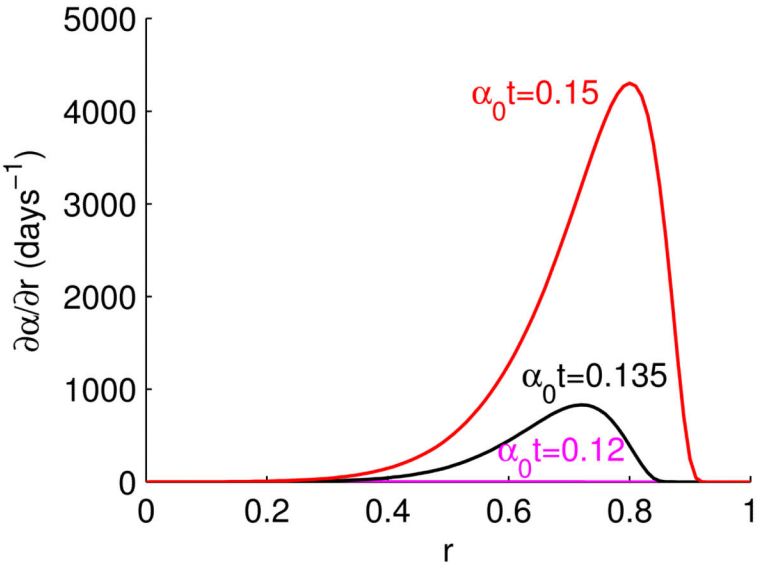

Figure 7.

Spatial derivative of diffusivity with respect to position r as a function of position for Case V ($\alpha = \alpha(f(r, t))$). The central difference approximations to the derivative are shown by solid curves at different times. The parameters are given in Table 1, and $\alpha_0 = D_b/R^2 = 2.1 \times 10^{-3}$ days^{-1}.

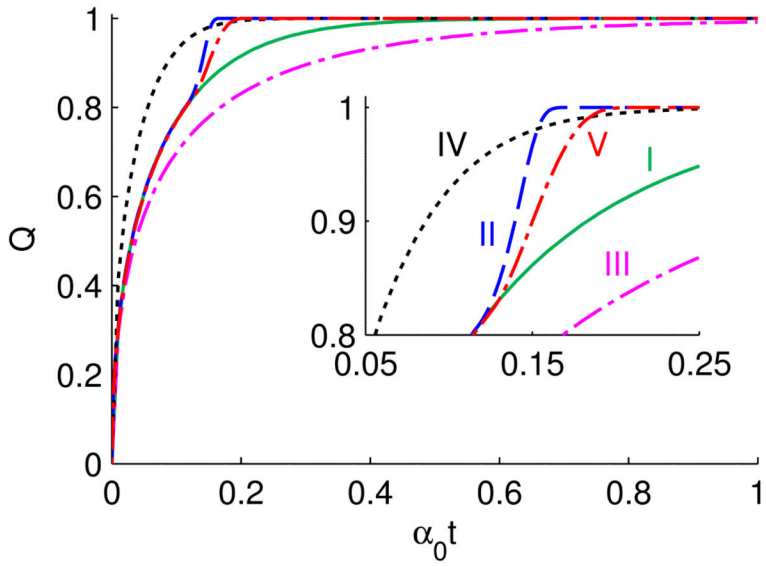

Figure 8.

Cumulative fraction released Q profiles as a function of dimensionless time $\alpha_0 t$ for Cases I–V. Analytical or semi-analytical solutions are shown for Cases I-IV, and the Scheme 1 numerical solution is shown for Case V. All cases have $\alpha_0 = D/R^2$, $D = 1.5 \times 10^{-13}$ cm^2/s, and $R = 25$ μm.

Table 1

Case V Parameters.

Parameter	Value	Units
D_b	1.5×10^{-13}	cm^2/s
D_∞	9.1×10^{-7}	cm^2/s
R	25	μm
R_d	36	Å
R_{p0}	0	Å
β	4.9×10^{-1}	Å
k	7.7×10^{-2}	day^{-1}
α_a	3.1×10^{-4}	day^{-1}
Φ_a	5π	
τ	3	

Table 2

Error, $||e||_2$, between the numerical solutions and the true solutions for diffusivity in Cases I–IV. Scheme 0 is shown as a baseline for comparison.

Case	$\|\|e\|\|_2$		
	Scheme 0	**Scheme 1**	**Scheme 2**
I	1.70×10^{-5}	1.70×10^{-5}	1.70×10^{-5}
II	3.81×10^{-5}	3.81×10^{-5}	3.81×10^{-5}
III	2.09×10^{-1}	2.72×10^{-4}	5.03×10^{-4}
IV	4.23×10^{-2}	1.80×10^{-5}	5.40×10^{-5}